New era of synchrotron radiation: fourth-generation storage ring

Seunghwan Shin

Abstract

There had been remarkable progress in developing third-generation electron storage rings as the main sources of very bright photon beams. Fourth-generation storage rings based on the multi-bend achromat lattice concept may be able to surpass the brightness and coherence that are attained using present third-generation storage rings. In this paper, we survey ongoing work around the world to develop concepts and designs for fourth-generation electron storage rings.

Keywords: Fourth-generation storage ring, Multi-bend achromat lattice, Brightness, Coherence

1 Introduction

High-brightness photon beams from storage rings play a central role in condensed matter material science and biology experiments in the world today. There are many outstanding characteristics of photon beams from storage rings: high brilliance and flux, wavelength tunability, beam size tunability, (partially) coherent radiation, polarization, time structure, etc. In addition, the photon beams are very stable in energy, intensity, position, and size.

There has been remarkable progress in developing electron storage rings over the last few decades. Figure 1 shows photon beam brightness from candle to X-ray free electron laser oscillator (XFEL-O) as a future light source. Photon beam brightness from storage rings has been dramatically increased since the advent of the first-generation storage ring. Here, brightness takes into account the number of photons per angular divergence, the cross-sectional area, and a bandwidth of 0.1% of photon beam as a figure of merit for storage ring.

In order to increase brightness, photon number can be increased by electron beam current and the enforced radiation source. In the third-generation storage ring, operation beam current has reached 400 mA or higher and undulator has been successfully operated to realize

dramatic increase of brightness. At the same time, the efforts have been made to reduce electron beam emittance for higher brightness.

The natural equilibrium emittance of an electron storage ring is determined by a balance between quantum excitation and radiation damping and given by

$$\varepsilon_0 = C_q \gamma^2 \frac{\langle \mathcal{H}/|\rho^3| \rangle}{j_x \langle 1/\rho^2 \rangle}, \qquad (1)$$

where C_q is a constant (for electrons $C_q \approx 3.832 \times 10^{-13} m$), γ is the relativistic factor for a particle, $\mathcal{H} \sim 1/\rho^2$ (where ρ is unit cell bending radius) and j_x is the horizontal damping partition number [2]. The progress in the design of the third-generation storage rings (3GSRs) leads to the natural equilibrium emittance nanometer range using the lattice design with double-bend achromat (DBA) lattice [3] or triple-bend achromat (TBA) lattice [4].

The natural emittance scales with the inverse cube ρ, so the multi-bend achromat (MBA) lattices [5] enabled emittance reduction by one to two orders of magnitude compared to third-generation storage ring. Storage rings based on MBA lattice concept are emerging as part of a worldwide push beyond the brightness and coherence reached by the present third-generation storage rings.

MAX-IV was the first MBA machine to be built and now in operation. It was followed shortly by SIRIUS [6]

Correspondence: tlssh@postech.ac.kr
Accelerator Division, PLS-II, Pohang Accelerator Laboratory, Pohang, Kyungbuk 37673, Korea
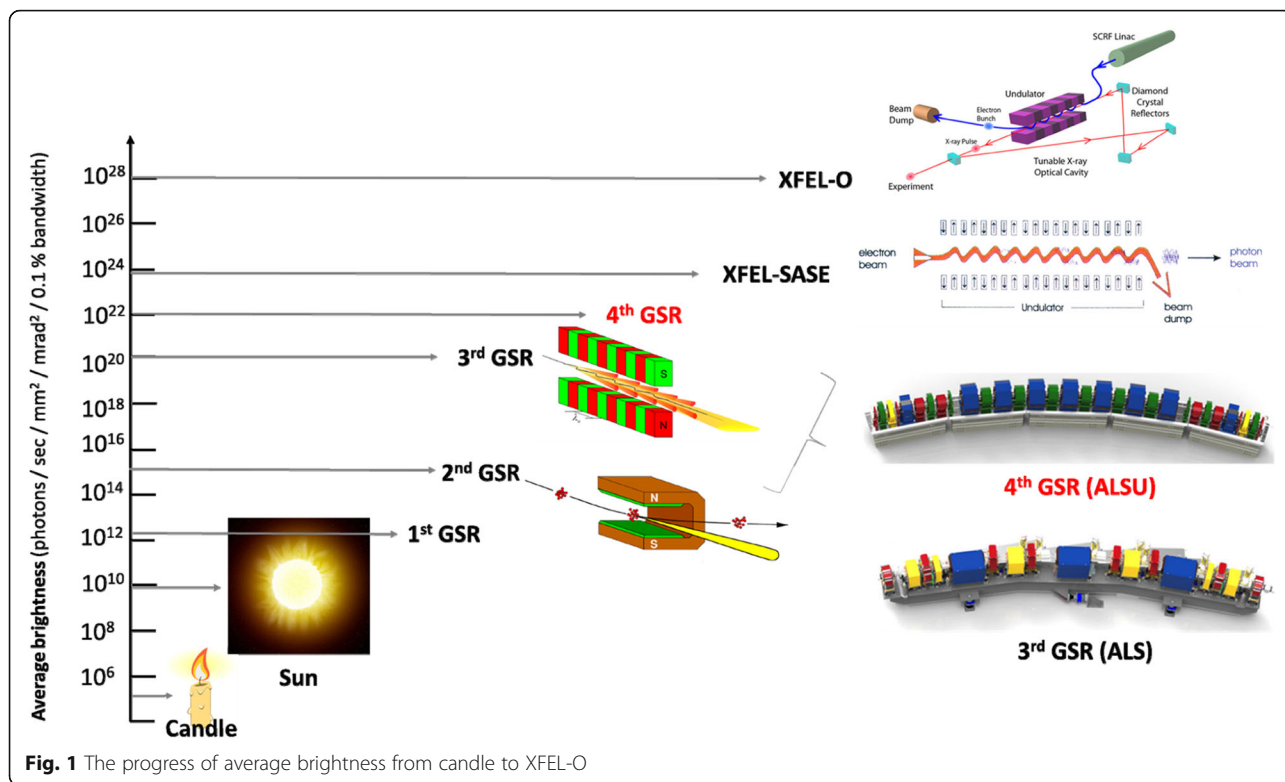
Fig. 1 The progress of average brightness from candle to XFEL-O

and European Synchrotron Radiation Facility Extremely Brilliant Source (ESRF-EBS) [7] which are also currently under operation. Other projects are underway to convert existing third-generation storage rings such as advanced photon source upgrade (APS-U), advanced light source upgrade (ALS-U), and PETRA-IV into fourth-generation storage rings. In the upgrade lattice designs for these facilities, the beam emittance is pushed down to a few hundred picometers, or even et100 pm. In this review paper, we address the new era of synchrotron radiation and describe overall contents about fourth-generation storage rings (4GSR).

2 Matured technology on 3GSR

From the early 90s, third-generation storage rings have been put into operation, producing highly brilliant radiation and specially optimized for the use of insertion devices. The ESRF was the first of the third-generation hard x-ray sources to operate. The ESRF has been followed by the APS at Argonne National Laboratory (7 GeV) in late 1996, and SPring-8 (8 GeV) in late 1997. These machines are physically large (850 to 1440 m in circumference) with a capability for 30 or more insertion device, and a comparable number of bend-magnet and beamlines. Among the low photon energy sources, the
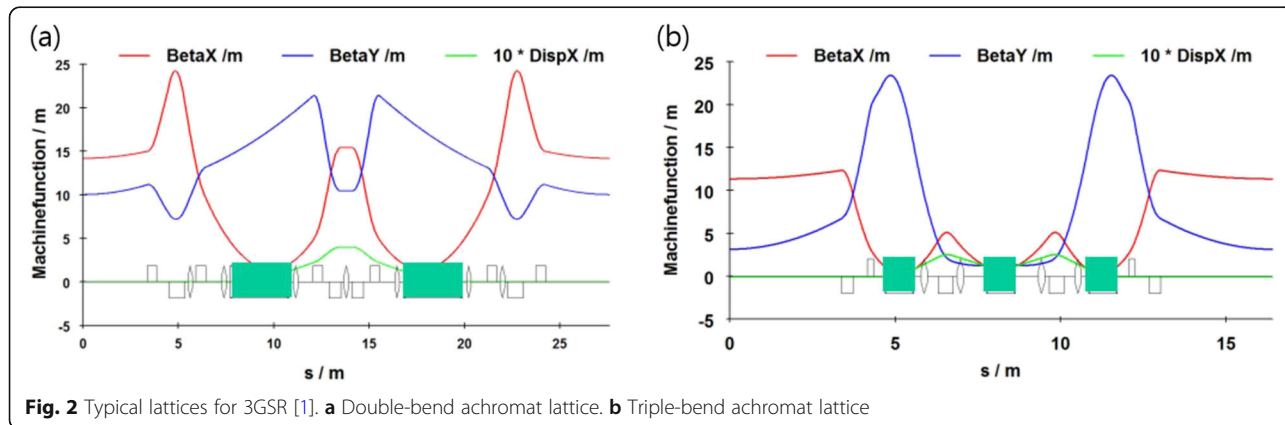

Fig. 2 Typical lattices for 3GSR [1]. **a** Double-bend achromat lattice. **b** Triple-bend achromat lattice

ALS at Berkeley (1.9 GeV) began its scientific program in early 1994, as did Electtra-Sincrotrone Trieste (Electtra, 2.0 GeV), followed by Taiwan light source (TLS, 1.3 GeV) and the Pohang light source (PLS, 2.0 GeV) [5]. Now, around 25 third-generation storage rings have been successfully operated worldwide and related technologies have been fully matured, and in this section, we will overview matured technologies as well as lattice design during 3GSR operation.

Recalling Eq. (1), the natural equilibrium emittance is scaling with the square of the beam energy, inversely with the partition number j_x, and is linearly proportional to the <H>. Here, <H> is the average of H evaluated in the bending magnets

$$< \mathrm{H} >= \frac{1}{2\pi\rho} \int \left[\gamma\eta^2 + 2\alpha\eta\eta' + \beta\eta'^2 \right] ds \qquad (2)$$

where α, β, and γ are the Courant-Synder parameters and η is dispersion function. For low-emittance storage ring design, we made effort to minimize the integral quantity <H>. Most 3GSR rings have adopted DBA lattice [3] or TBA [4] as lattice option (Fig. 2). In Eq. (2), it is clearly seen that <H> depends on lattice functions. With optimum lattice functions, the minimum emittance of the DBA lattice is given by [5]

$$\varepsilon = \frac{94.95 \; nm \; rad}{J_x} \left(\frac{E}{GeV} \right)^2 \left(\frac{\phi}{rad} \right)^3 \varepsilon$$
$$= \frac{94.95 \mathrm{nmrad}}{J_x} \left(\frac{E}{GeV} \right)^3 \left(\frac{\phi}{rad} \right)^3 \qquad (3)$$

where ϕ is bending angle. The minimum emittance of TBA lattice with satisfying achromatic condition is [5]

$$\varepsilon = \frac{73.85 \; nm \; rad}{J_x} \left(\frac{E}{GeV} \right)^2 \left(\frac{\phi}{rad} \right)^3 \varepsilon$$
$$= \frac{73.85 \mathrm{nmrad}}{J_x} \left(\frac{E}{GeV} \right)^3 \left(\frac{\phi}{rad} \right)^3 \qquad (4)$$

Later, most 3GSRs adopt finite dispersion in the straight section without keeping achromat condition and realize smaller emittance than emittance with achromat condition. Emittances for 3GSRs distribute a few nanometer ranges.

Top-up injection refers to injecting with photon shutters open to deliver a near-constant stored beam current [8]. In order to stabilize the stored electron beam orbit as well as the synchrotron radiation flux, a small amount of beam current had to be injected into the stored beam to keep its current almost constant during top-up operation. Now, top-up injection is the standard mode of operation in the third-generation storage ring after decay mode injection in the early 2000.

In order to extend spectral range for low-energy storage ring, several technologies have been matured during operation of the third-generation light source. Super-bend concept (high magnetic field-bending magnet) was applied in storage ring. For instance, the radiation produced by 5T super-conducting magnets at is an order of magnitude higher in photon brightness and flux at 12 keV, making them excellent sources of hard X-rays for protein crystallography and other hard X-ray applications in ALS [9]. The other is short-period in-vacuum undulator concept (Fig. 3) to generate higher photon beam spectrum. In the meantime, effort to use higher undulator harmonics had been made. As result, up to 21-keV undulator radiation using 11th harmonic is obtained and available at undulator beamline [10].

Experimental physics and industrial control system (EPICS) [11] had been rooted as control system in third-generation storage rings. As result, a standard tool-kit for accelerator control system and many applications are available through worldwide collaboration. In addition, digital control system for magnet power supply and electronics is a general trend. It enables control system to be less sensitive to noise, to do easy return to original settings, and to do easy replacement of malfunction component. Theses control system in the third-generation light source contributes to high accelerator machine reliability (say, higher than 97% beam availability).

Stability of electron orbit is one of the most important properties to achieve brilliant photon beams for third-generation storage ring [12]. With many efforts such as suppression on noise source, insertion device feed-forward (ID FF) [13], and fast orbit feedback implementation, orbit stability has been achieved within several microns per day up to 100 Hz motion.

As mentioned above, many technologies had been established as the general trend during the operation of third-generation storage rings. On the other hand, some technology options are still compatible to be applied in accelerator development. As injector for storage ring, booster ring is main option but linear accelerator is candidate on injector with potential capability for free electron laser (FEL) application [14] (Fig. 4). In Fig. 5, it will also be a difficult choice to discriminate between normal cavity and super-conducting cavity options.

3 The beginning of 4GSR
It should be noted that MBA lattice concept is not recent idea but was already introduced in 1993 [15, 16]. Theoretical minimum emittance (TME) with optimal condition [6] is
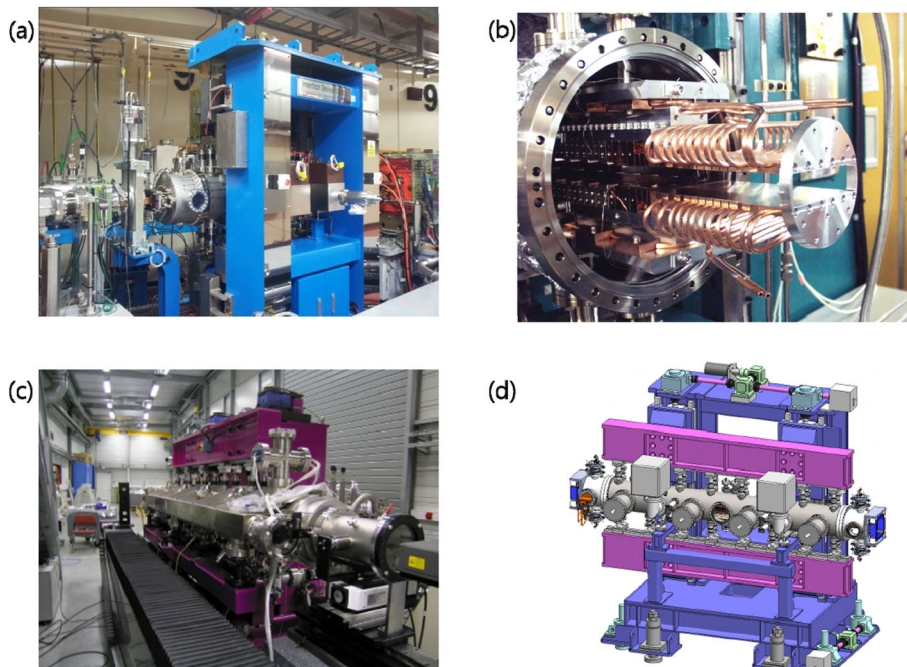
Fig. 3 In-vacuum undulator in 3GSR. **a** In-vacuum undulator in PLS-II. **b** In-vacuum undulator in ALS. **c** Cryogenic in-vacuum undulator in ESRF. **d** In-vacuum undulator in TPS

$$\varepsilon = \frac{31.65 \; nm \; rad}{J_x} \left(\frac{E}{GeV}\right)^2 \left(\frac{\phi}{rad}\right)^3 \qquad (5)$$

Compared with DBA and TBA lattice in Eqs. (3) and (4), TME can reach emittance with a factor of two less. In case of MBA lattice, the minimum emittance with optimal condition [17] is $\varepsilon = \frac{73.85 nmrad}{J_x} \left(\frac{E}{GeV}\right)^3 \left(\frac{\phi}{rad}\right)^3$

$$\varepsilon = \frac{31.65 \; nm \; rad}{J_x} \left(\frac{M+1}{M-1}\right)\left(\frac{E}{GeV}\right)^2 \left(\frac{\phi}{rad}\right)^3 \qquad (6)$$

where M is number of bending magnets in cell. Here, the central bending magnets should be longer than the outer bending magnets. In addition, the lattice functions in the outer dipoles are the same as in a DBA lattice and in the inner dipoles are the same as in a TME lattice. From Eq. (6) and Fig. 6, MBA concept is to minimize emittance by reducing magnet angle in Eq. (6) and reaching TME.

Initial lattice design for Swiss light source (SLS) is followed with MBA concept. The lattice provides small emittance 3.2 nm with 252-m circumference at 2.1 GeV.
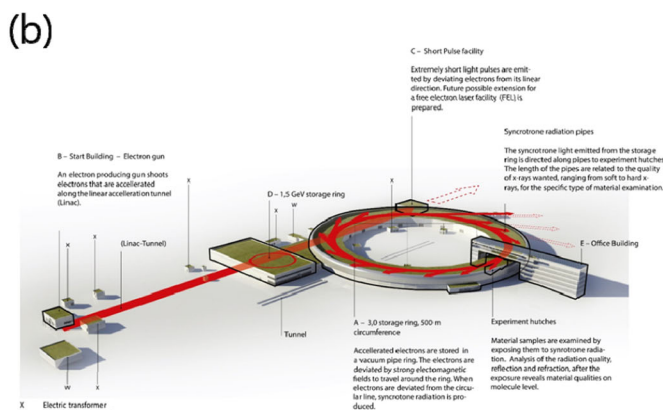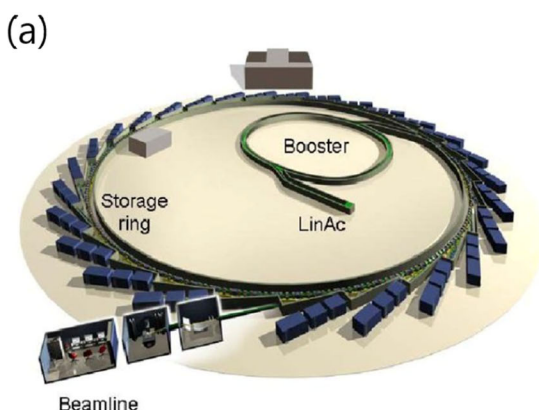

Fig. 4 Injector system for 3GSR. **a** Booster. **b** Linear accelerator
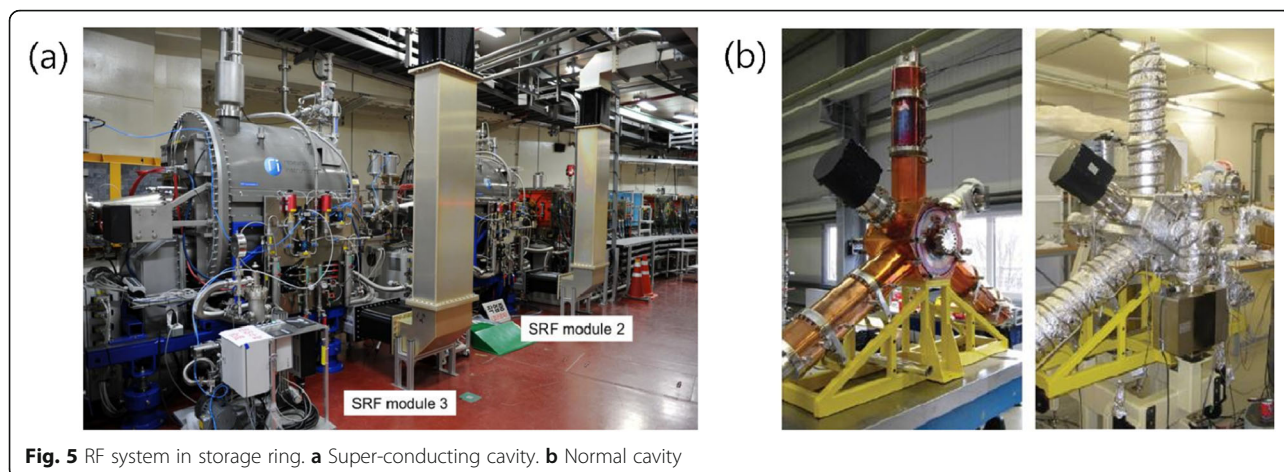
Fig. 5 RF system in storage ring. **a** Super-conducting cavity. **b** Normal cavity

However, facing hardware challenges, 5.5-nm emittance SLS storage ring with TBA lattice was actually built with 280-m circumference at 2.4 GeV. Key components for realizing compact lattice for 4GSR needed to be resolved from technical challenges at that time.

The MAX laboratory inaugurated MAX-III, a 700-MeV storage ring in 2007. Technical challenges for compact machine were initially demonstrated in MAX-III. As shown in the Fig. 7, MAX-III realized the integrated magnet system which could make machine compacter. In the meantime, some pioneering laboratories such as SOLEIL, MAX Laboratory, and SIRIUS started extensive use of non-evaporable getter (NEG)-coated chamber for their storage ring vacuum system, which had been developed in CERN. The NEG coating provides a low photon-stimulated gas desorption and sticking of active gases resulting in low operating pressure in a storage ring with a small aperture. As a result, compared with 3GSR, vacuum chamber for 4GSR is much smaller in Fig. 8.

Based on these environments, eventually, the MAX-IV [19] 3-GeV electron storage ring was started, the first of a new generation of light sources to make use of MBA lattice to achieve ultralow emittance and hence ultrahigh brightness and transverse coherence.

4 Overview of worldwide 4GSRs
After the MAX-IV as the first 4GSR successfully started operation, it was be followed by SIRIUS [20] and ESRF-EBS [21], which are also currently under operation. Other 4GSR construction projects, such as the APS-U [22] and ALS-U [23], are proceeding with the upgrades of the existing 3GSRs into 4GSRs, and other new 4GSR construction projects, such as high-energy photon source (HEPS) [24], are also under progress. Moreover, many existing synchrotron radiation accelerators are scheduled for upgrade into 4GSRs, and active research studies for new 4GSR projects are underway. In the 4GSR lattice designs for these facilities, the beam emittance is pushed down to a few hundred picometers or
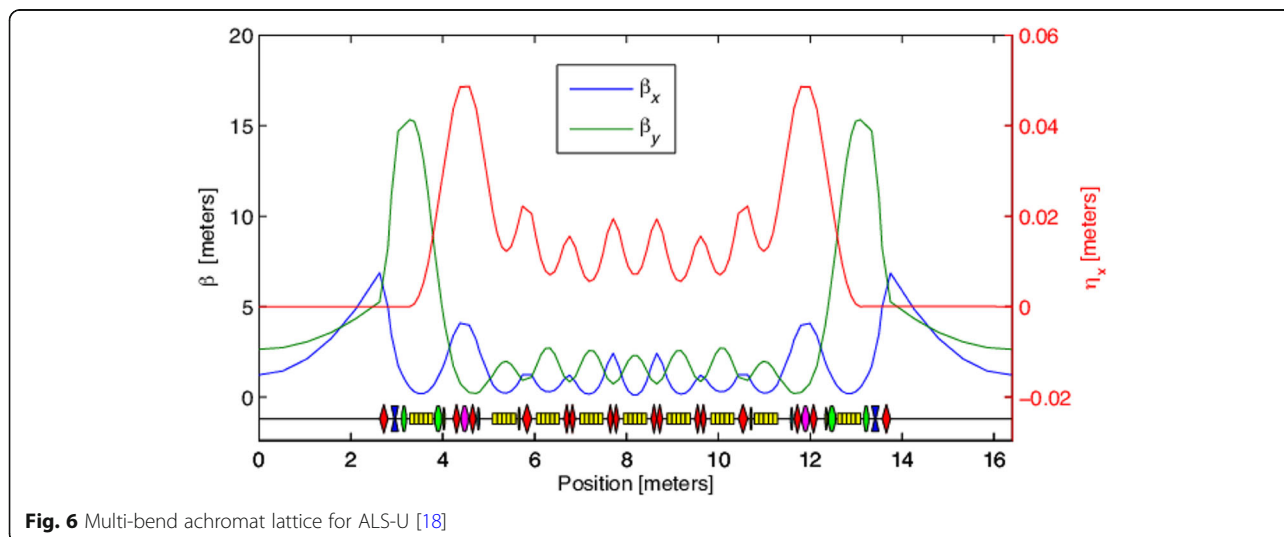

Fig. 6 Multi-bend achromat lattice for ALS-U [18]

Fig. 7 Compact unit cell in MAX-III

even < 100 pm. In this section, we overview the present status of worldwide 4GSR. Characteristics on 4GSR are also described in this section.

Brilliance and coherent fraction are the key performance parameters for 4GSR. Brilliance, defined as the ratio of the photon spectral flux to the volume of the convoluted phase of the electron beam and the photon beam in the two transverse dimensions, is given by

$$\text{Brilliance} = \frac{flux}{4\pi^2 \Sigma_x \Sigma_{x'} \Sigma_y \Sigma_{y'}} \tag{7}$$

where the convoluted sizes and divergences are

$$\Sigma_x = \sqrt{\sigma_{x,e}^2 + \sigma_{ph}^2}, \Sigma_{x'} = \sqrt{\sigma_{x',e}^2 + \sigma_{ph}'^2} \tag{8}$$

Here $\sigma_{x,\ e}$, σ_{ph}, $\sigma_{x',e}$, and σ_{ph}' are electron beam size, photon beam size by single electron, electron beam divergence, and photon beam divergence by single electron, respectively. Coherent fraction, defined as the ratio of the photon wavelength to the volume of the
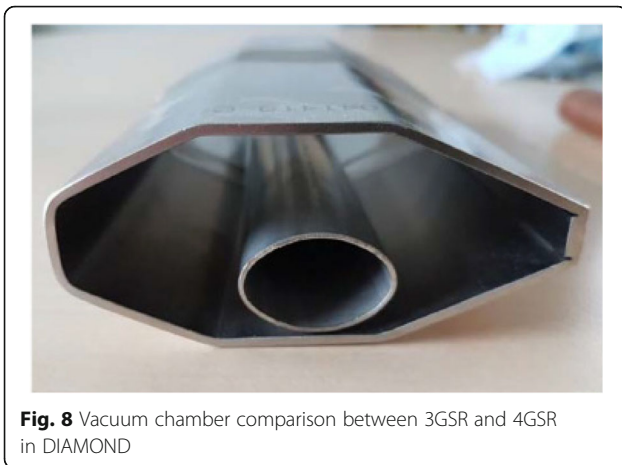

Fig. 8 Vacuum chamber comparison between 3GSR and 4GSR in DIAMOND

convoluted phase of the electron beam and the photon beam in the two transverse dimensions, is also given by

$$F = \frac{\lambda^2/(4\pi)^2}{\Sigma_x \Sigma_{x'} \Sigma_y \Sigma_{y'}} \tag{9}$$

Therefore, brilliance and coherent fraction are maximized for smaller electron beam emittances until the diffraction limit is reached. As typical values, around 10 pm electron emittance can reach diffraction limit at around 1 Å (12.4 keV).

Figure 9 shows distributions of low-emittance rings including 4GSR along the ring circumference. Vertical axis in the figure indicates natural emittance normalized by the square of energy. Facilities with blue color indicate 3GSR with DBA or TBA lattice concept. It is clear that natural emittance is reducing along the cubic of circumference from the distribution of 3GSR. By implementing MBA lattice concept and compact technology, 4GSR with red color obtains 100 times emittance reduction (or even more) than 3GSR. Considering on-axis injection scheme, reverse bends, and cutting-edge technology, emittance is pushed into 3~4 times smaller. Ultralow emittance rings such as HEPS (< 60 pm), Korea-4GSR (58 pm), APS-U (42 pm), and PETRA-IV (20 pm) provide high brightness and coherence up to high photon energies.

Currently, mainly three kinds of multiband concepts are adopted on lattice design for 4GSR: classical multi-bend achromat (Fig. 10), hybrid multi-bend achromat (Fig. 11), and variated multiband achromat (Fig. 12). Most of the classical multiband achromat lattices implement seven bends per cell. The classical seven multiband achromat lattice consists of unit cells, which are close to theoretical minimum emittance lattice, and matching cell, which make dispersion zero at straight section. Here, one cell consists of a five-unit cell in the central region and two matching cells at the edge side. As an example, MAX-IV, SIRIUS, and SLS-II adopt the classical multiband achromat lattice. Here especially, SLS-II started to consider unit cell with uncommon magnet such as longitudinal gradient magnet and reverse bend magnet to realize lower emittance than theoretical minimum emittance. Sextupoles are distributed along the cell in the classical multiband achromat lattice.

Hybrid multiband achromat lattice originates from the need of low-emittance rings for the SuperB project. In 2012, there was immediate interest and enthusiasm on the potential of the SuperB lattice design for 4th-generation storage ring at ESRF. ESRF-EBS is the first hybrid multi-bend achromat (HMBA) machine. The HMBA lattice features as follows: (1) multi-bend for lower emittance, (2) dispersion bump for efficient chromaticity correction and thus weak sextupoles, (3) fewer
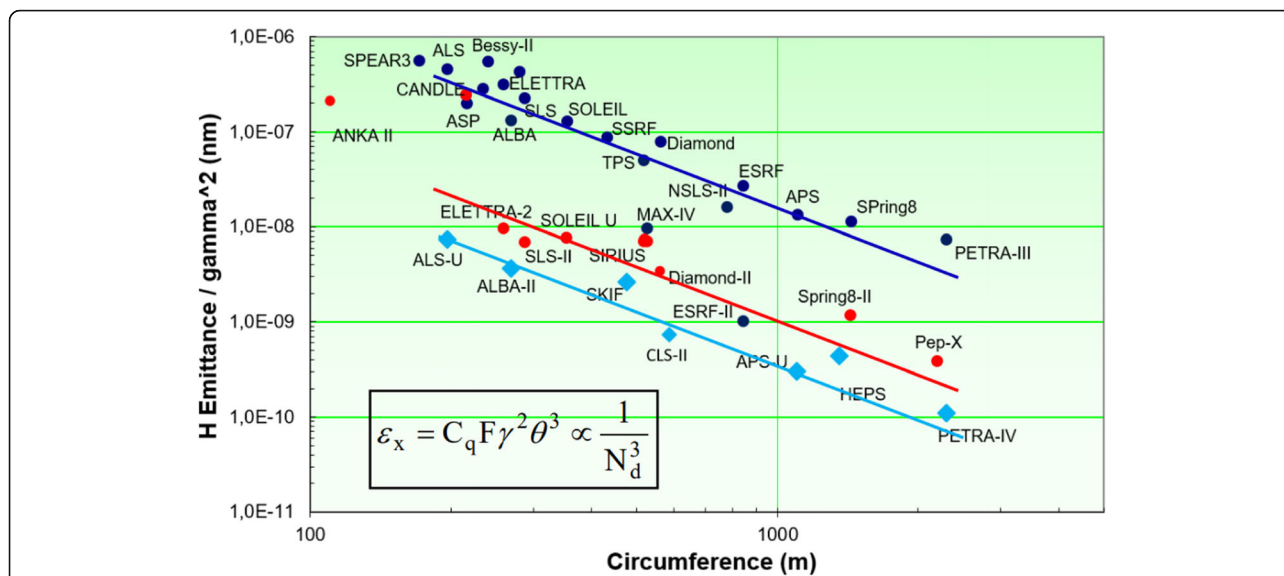
Fig. 9 Storage ring distributions along circumference [25]

sextupoles, and (4) longer and weaker dipoles. Currently, APS-U, HEPS, PETRA-IV, and Korea-4GSR adopt HMBA concepts and improve the lattice performance to realize lower emittance and larger dynamic aperture.

Besides the classical MBA and HMBA, modified HMBA is adapted to a few machines. DIAMOND started the concept double-double-bend achromat (DDBA) providing an additional straight section in the middle of the arc such as SOLEIL and PLS-II. Later, DIAMOND-II merges the concepts of the HMBA cell design for the ESRF-EBS with the DDBA. The resulting lattice is a modification of the 7BA lattice of the ESRF-EBS where the middle dipole has been

removed to create a mid-straight section and the adjacent gradient dipole magnet tuned to control the optics functions. The performance of this lattice in terms of dynamic aperture and momentum aperture is compatible with the considering of an off-axis injection [26].

Table 1 shows ring parameter summary of worldwide 4GSR projects. Energies of storage ring are distributed from 2 to 6 GeV. Their emittances are below 300 pm and PETRA-IV shows minimum emittance as 20 pm by help of large circumference. The trend of 4GSR lattice design is to consider implementing reverse bends. It should be noted that not all machines realize beta-
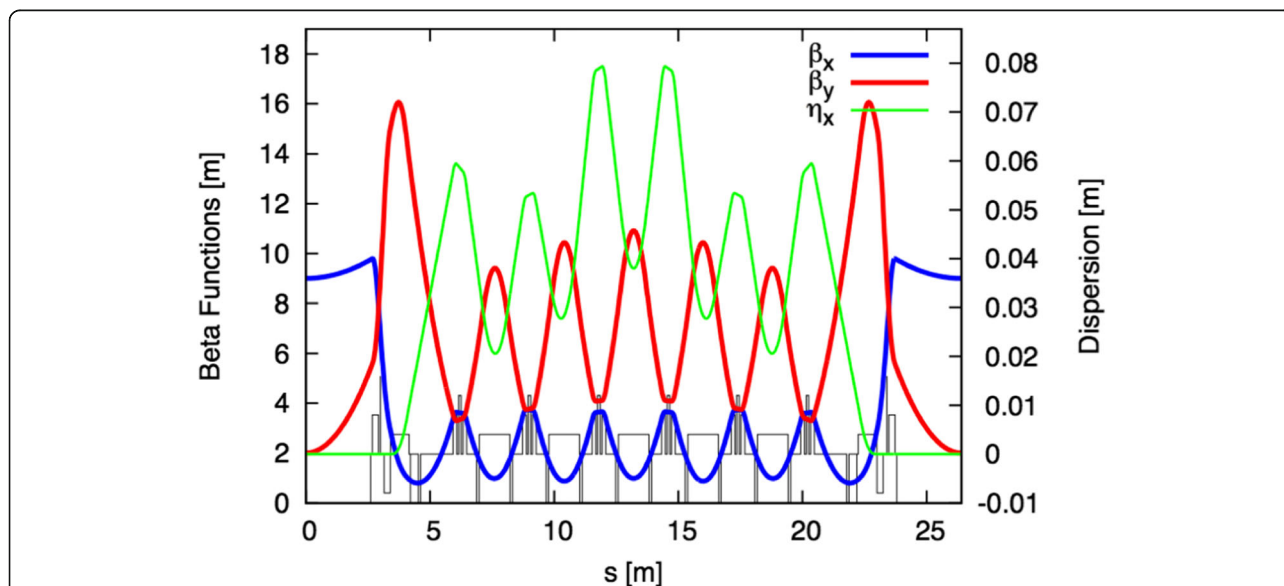

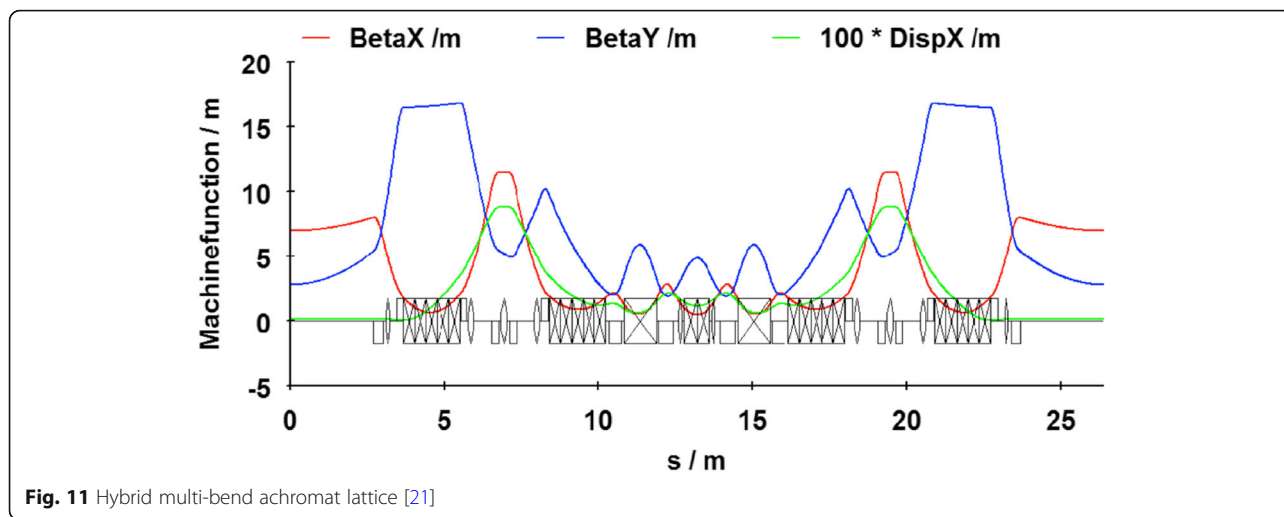**Fig. 10** Classical multi-bend achromat lattice [19]

Fig. 11 Hybrid multi-bend achromat lattice [21]

function optimization for matching phase space between electron beam and photon beam. Only several machines have large horizontal beta-function at injection point for easy beam injection.

High gradient magnets used in 4GSR are summarized in Table 2. The lattice design of 4GSR relies on the use of strong focusing quadrupoles with gradients up to 100 T/m. These magnets require a very small-bore aperture to achieve the high design field. The magnet cross-section and length have been also driven by a complex engineering integration, considering clashes with the photon extraction pipe, adjacent magnets, and other lattice elements such as flanges, gate valves, vacuum pumps, absorbers, and BPMs. Most 4GSR machine will consider octupole to control higher order chromatic effect. Use of longitudinal gradient magnet is necessary to reduce emittance further. Permanent magnet design is considered an alternative choice for sustainability.

Sensitiveness to alignment errors at low-emittance ring requires a careful study of the alignment tolerances. Beam-based methods are commonly exploited and in the recent years the so-called commissioning simulations have been used in defining the acceptable limits for magnet and girder alignments. Table 3 shows alignment tolerance for worldwide 4GSR facilities and compares tolerance requirement with 3GSR. It should be remarkable that the required tolerance levels for 4GSR are similar with those of 3GSR due to a more elaborated approach with beam-based methods and extensive computations.

The design lattice parameters during commissioning will need to be quickly achieved in order to minimize commissioning period. Accelerator physics developed and used start-to-end simulation of the machine commissioning beginning from first turn trajectory correction, progressing to orbit correction, and culminating
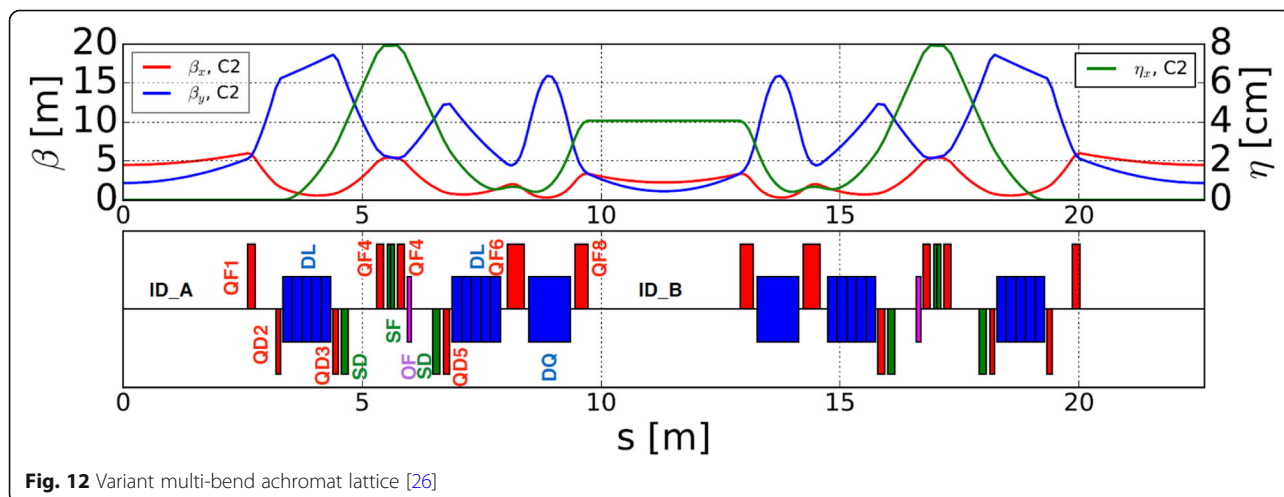

Fig. 12 Variant multi-bend achromat lattice [26]

Table 1 Worldwide ongoing 4GSR projects [25]

	Energy (GeV)	Emittance (pm)	Ener. spr. (1e− 4)	Beta x/y (m) @ source point	DA (mm)/beta x (m) @ inj. point	LMA (%)/TL (h)	Mcf (1e− 5)	Reverse bends	ID source point move
ALS-U	2.0	108	9.8	2.0/2.8	1.0/2.0	2.5/1.0	27	Yes	No
ELETTRA 2	2.4	212	9.3	5.7/1.6	6.0/5.7	4.0/6.2	12	Yes	No
SLS-II	2.7	157	12.0	2.5/1.3	7.0/22.0	4.0/6.3	10.4	Yes	< 70 mm
SOLEIL-U	2.75	81	9.0	1.3/1.3	5.0/11.0	3.5/3.3	9.1	Yes	< 100 mm
SIRIUS	3	250	8.5	1.5/1.5	10.0/17.0	3.7/3.9	16.0	No	n/a
Diamond-II	3.5	136	9.0	6.0/2.5	5.0/6.0	1.6/4.0	11	Yes	No
APS-U	6	42	13.5	4.9/1.9	2.2/5.2	2.1/4.0	4.0	Yes	No
ESRF-EBS	6	135	9.3	6.9/2.6	8.0/18.6	3.4/20	8.5	No	No
HEPS	6	< 60 (35)	10	2.6/2.3	1.0/2.6	1.5/1.0	1.8	Yes	n/a
PETRA-IV	6	20	11.2	4.0/2.0	3.6/21.7	2.0/1.2	1.6	tbd	Yes

in lattice correction and coupling adjustment. The automated commissioning procedure shows that the rapid commissioning of the ultralow-emittance lattice is possible. Figure 13 shows the result of simulation tool and the summary of all correction step in commissioning is introduced in the reference [27].

Recently ESRF-EBS (140 pm, 6 GeV 4GSR) had achieved the nominal operational parameters ahead of schedule by help of robust lattice design, relatively conventional technologies and elaborated commissioning tool. The brief milestones of the ESRF-EBS commissioning are as follows:

– 28 November 2019: Start of commissioning (3 turns)
– 06 December 2019: First stored beam (Fig. 14)
– 15 December 2019: First accumulation
– 14 March 2020: 200 mA beam store

The commissioning of the ESRF-EBS had been extremely successful and on August 25, 2020, user service mode operations started as planned. In addition to MAX-IV and SIRIUS, the first 6-GeV dream machine

had come to life and delivered ultra-small X-ray beams (Fig. 15).

5 Issues and technologies on 4GSR

In this section, general description and issues on technologies for 4GSR will be discussed. Firstly, the 4GSR lattice features many magnets in the lattice space compared to 3rd-generation light sources. Therefore, magnets in 4GSR lattice are very crowded with minimal space between the magnets which is challenging for installation and maintenance. The lattice space should be also precisely modeled in 3D to avoid any mechanical interference with other magnets, vacuum, and diagnostic components. Secondly, the magnetic strengths of quadrupole magnets are stronger than the previous generation. To achieve this, the magnet aperture is reduced to 10~15 mm, and the pole tip field is increased to 1.12 T to maximize the field gradient. Since the magnetic properties of magnet still did not improve in previous 30 years, the increase in the pole tip field is a significant challenge. Thirdly, magnets became more complicated requiring longitudinal gradient in beam direction, or

Table 2 Magnet field summary for 4GSR [25]

	Energy (GeV)	MAX b′ (T/m)	MAX b″ (T/m²)	MAX b‴ (T/m³)	Min. bore radius (mm)
ALS-U	2.0	105	10,500	n/a	12.0
ELETTRA 2	2.4	50	4000	45,000	13.0
SLS-II	2.7	97	8000	270,000	10.5
SOLEIL-U	2.75	< 110	16,000	1,500,000	8.0
SIRIUS	3	45	2400	n/a	14.0
Diamond-II	3.5	85	7700	660,000	12.0
ESRF-EBS	6	90	3200	37,000	12.8
HEPS	6	80	7500	670,000	12.5
PETRA-IV	6	92	6400	330,000	12.5
APS-U	6	86	6300	n/a	13.0

Table 3 Alignment tolerance for 4GSR [25]

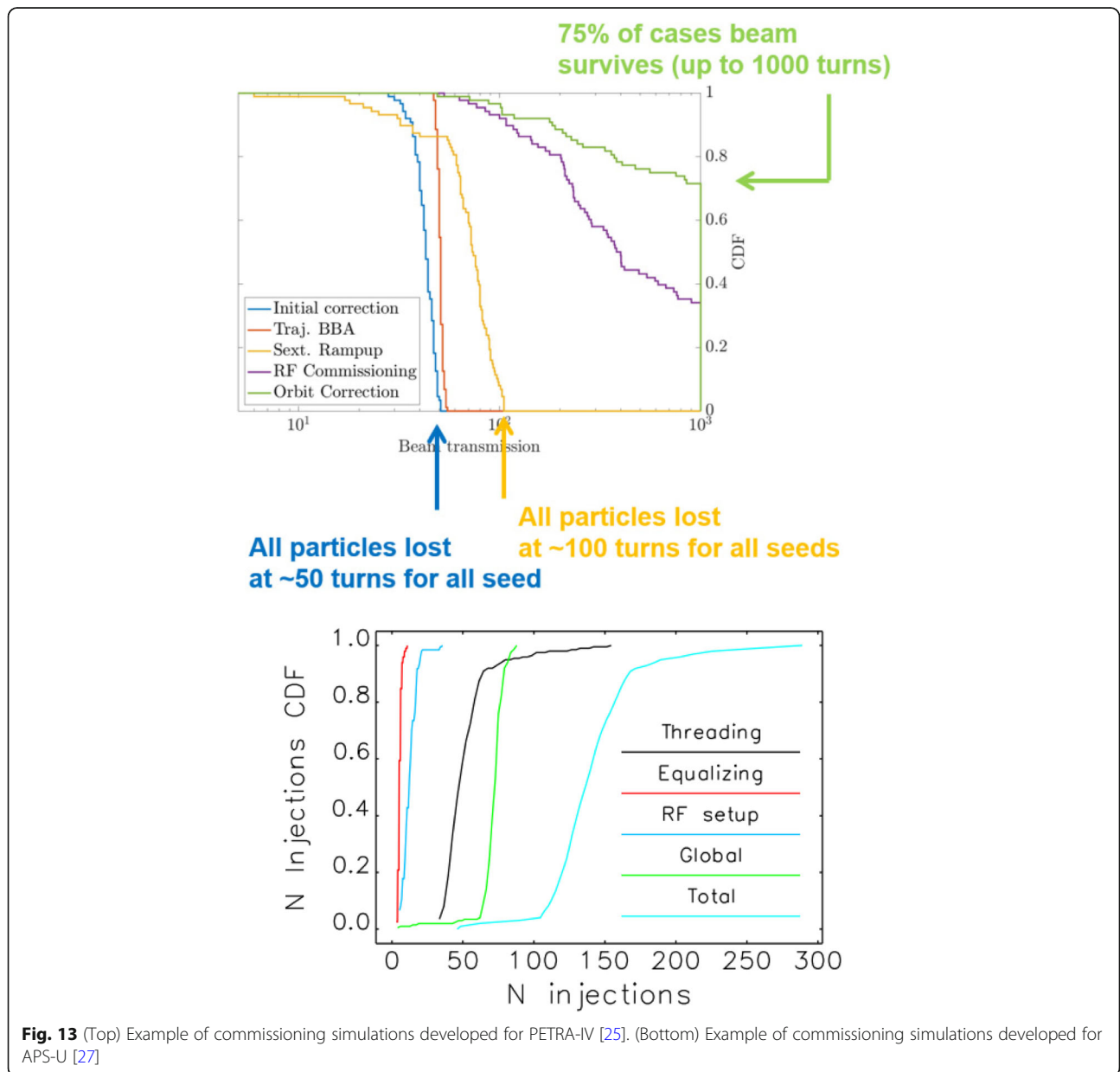|	Emittance (pm)	Magnet-to-girder offset (μm)	Girder-to-girder offset (μm)	Girder-to-girder roll (μrad)
ALS-U	108	20	50	100
ELETTRA2	212	20	50	100
SLS-II	157	30	60	100
Diamond-II	136	30	100	200
SIRIUS	250	40	80	300
APS-U	42	30	100	400 (magnets)
ESRF-EBS	135	60	ESRF measured	200 (magnets)
PETRA-IV	20	30	50-100	100
3GSR	Few*1000	30	100	200

Fig. 13 (Top) Example of commissioning simulations developed for PETRA-IV [25]. (Bottom) Example of commissioning simulations developed for APS-U [27]

Fig. 14 Picture taken in the control room with Pantaleo Raimondi, Accelerator Division Director, and his team, checking the first stored beam

requiring operation in offset position in quadrupole. In the previous 3rd-generation synchrotron light source, combined dipole is usually achieved adding smaller quadrupole component in dipole geometry. In 4GSR, dipole bending (or anti bending) is achieved using offset operation in quadrupole configuration which is more challenging since the dipole component depends on the offset position.

Main features of 4GSR vacuum systems are small aperture for beam chambers and tight space for vacuum instruments in order to accommodate required number of magnets. Some pioneering laboratories such as SOLEIL [28], MAX-IV [29], and SIRIUS [30] succeeded

in extensive use of NEG-coated chamber for their storage ring vacuum system, which had been developed in CERN. The NEG coating technology provides low photon-stimulated gas desorption and effective sticking capacity for major residual gases, which enables achieving required vacuum level in the small aperture vacuum system with the tight space. Recently, a vacuum chamber with an inner diameter of 6 mm has been reported to be successfully NEG-coated using pulsed magnetron sputtering [31]. There was a study on the compromise between maximizing gas pumping ability and minimizing the resistive wall impedance, which depends on the thickness of the NEG coating [32].
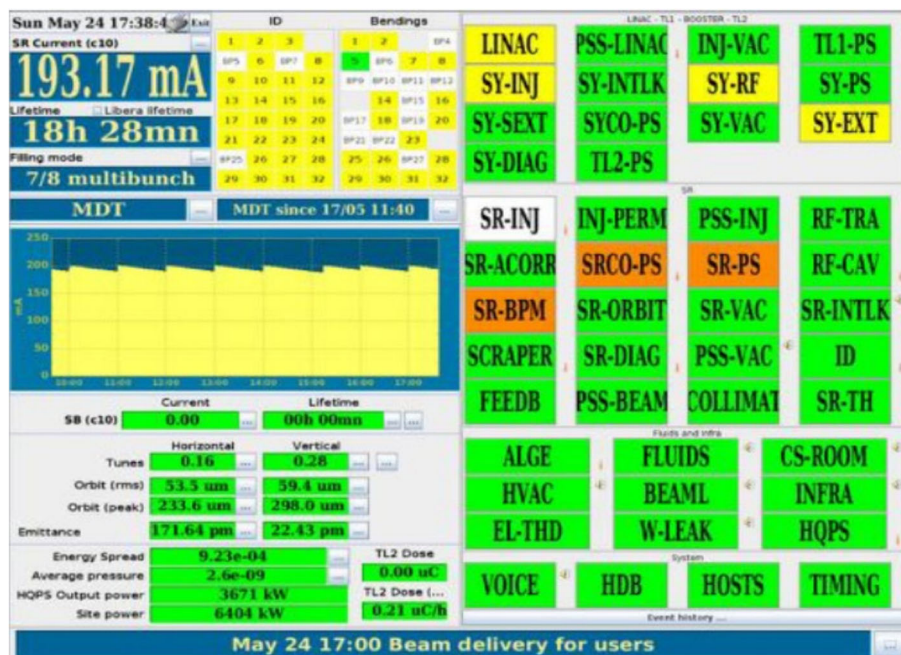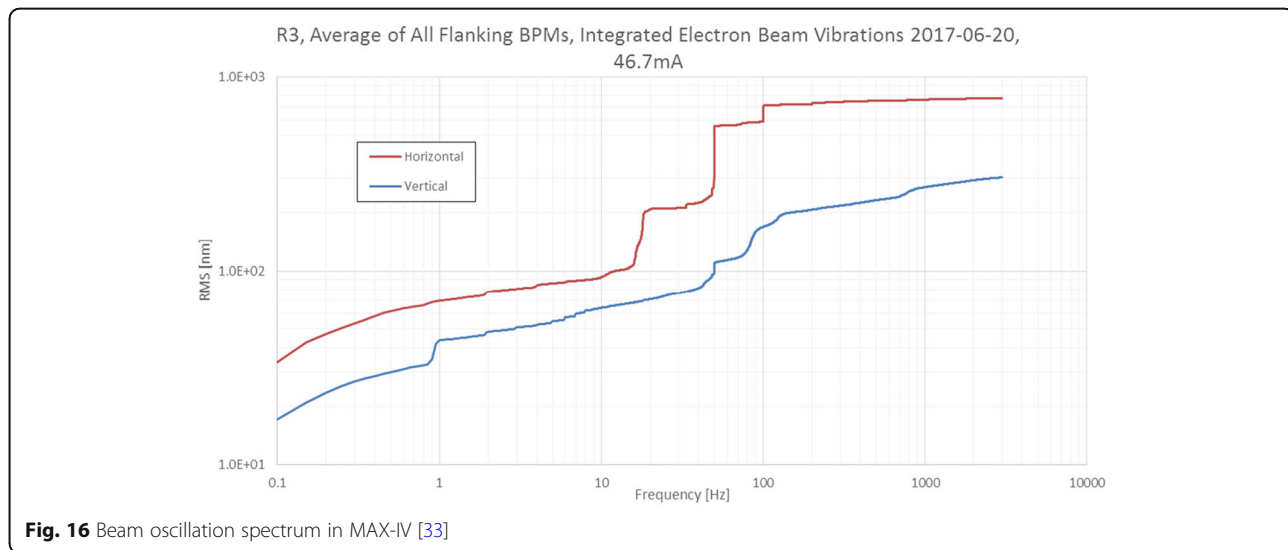

Fig. 15 Commissioning status of ESRF-EBS in 2020

Fig. 16 Beam oscillation spectrum in MAX-IV [33]

For 4GSR, beam stability should be also studied with extensive work scope. Users need stable photon beam for several prospects: brilliance, position, polarization, coherence, etc. To satisfy them, storage ring should maintain a stable electron beam. Due to the ultralow emittance and strong magnet fields of 4GSR, stability tolerances of the storage ring and beamline is tighter than the tolerances of 3GSR. Therefore, beam stability should be considered during the entire construction from the civil engineering stage to the beamline optics arrangements. In the case of MAX-IV, the stability task force was established to collect the efforts on stability during machine development, installation, and building construction. As a result, beam oscillation is maintained below 1 μm for both x and y positions up to 1 kHz (Fig. 16). In addition, the overall active systems like an orbit feedback should be also used carefully. In case of APS-U, corrector power supply set-point rate in fast orbit feedback increase up to 22.6 kHz from 1.6 kHz in the present APS system to maintain a low-emittance electron beam.

Realization of such characteristics as mentioned above (i.e., few micro-meters beam size and small aperture vacuum chambers) requires technological evolution which means more fast, reliable, and operational diagnostic system than that utilized in 3GSR. Most diagnostics of 3GSR such as beam current, bunch length, and filling pattern can be used in 4GSR with minor upgrades; however, a few diagnostic devices have technical challenge to be overcome. The beam size that is close to the diagnostic resolution limit caused not only the difficulty of diagnosis itself but also increment in sensitivity of beam vibration together with the small aperture vacuum chamber. To handle such sensitive conditions, the processing platform should feedback and control faster, the signal strength of

the hardware should be enlarged, and the drift of measurement in time should be lowered, 10–100 times, respectively. Such sensitive conditions apply similarly to a photon beam diagnostic. A thin and small size diamond pixel detector and a very fast (up to 1 kHz) photon beam position feedback system has been developing and utilizing to handle the smaller and brighter X-rays of 4GSR.

Many R&D activities at various facilities on novel insertion device concepts are currently being carried out. A cryogenic permanent magnet undulator (CPMU) is widely proposed in many laboratories as the most popular undulator type in R&D activities. In addition to CPMU, super-conducting undulator and a symmetric design with the gap as small as the slit (DELTA) undulators are also actively studied. In order to obtain high brilliance at high photon energy, short periods, and small gap undulator is required in the 4GSR. A CPMU is suitable as a short-period undulator because of the high resistance to synchrotron radiation damage due to high material coercivity at low temperatures and because of the low beam-induced thermal load due to the reduction in the image current heating of the magnet cover by 2–3 times compared with room temperature. However, low gap operation is a key topic including resistive wall impedance and radiation damage with short lifetime in many operating modes. The summary of major IDs R&D is as follows [25]:

- ALS-U: Advanced planar polarized light emitter-X (APPLE-X) undulators 8.5-mm gap; in-vacuum undulator at 4.0-mm gap
- APS-U: Hybrid permanent magnet undulator (HPMU) at 8.5-mm gap; super-conducting undulator (SCU) at 8.0-mm gap

– Diamond-II: In-vacuum undulator to 4.0-mm gap
  and CPMUs but also SCUs and Apple-II-Knot
– ESRF-EBS: In-vacuum undulator to 6.0 mm gap and
  CPMU with 18 mm and 6.0 mm gap
– HEPS: CPMU at 5.2-mm gap
– SIRIUS: DELTA-type undulators 21-mm period and
  7.0-mm gap
– SLS-II: SCUs 10-mm period, 3.6-mm gap; SPMU
  14-mm period, 4.0-mm gap
– SOLEIL-U: CPMU 12–18-mm period, 4.0-mm gap;
  APPLE-III, two period EPU and APU

Strong sextupole in the 4GSR will significantly reduce the dynamic apertures, and this is a great challenge for 4GSR lattice design, leading to severe difficulties for injection. Figure 17 shows storage ring acceptance along emittance. In the figure, it is clear that dynamic aperture (dynamic transverse acceptance) is small for low-emittance ring and on-axis injection should be considered in dynamic aperture regimes below roughly 3-mm mrad. "Swap-out" injection [34] as typical on-axis injection scheme uses a fast dipole kicker to inject a fresh high-charge beam onto the closed orbit while the stored beam is extracted. Figure 18 shows the schematics of swap-out on-axis injection in HEPS. Compared with dynamic aperture, momentum acceptance is also still some percent for low-emittance ring (i.e., momentum acceptance depends weakly on emittance) in Fig. 19. That causes the recent trend toward longitudinal injection. Figure 20 shows summary of injection schemes proposed or developed so far. For 4GSR,

various longitudinal injection schemes have been proposed. These longitudinal injection schemes are being considered on-axis injection in transverse planes but off phase or off energy injection in longitudinal plane in order to overcome the problem on small dynamic aperture.

6 4GSRs in Asia

In this section, we briefly introduce 4GSR projects in the Asia region. Some activities on accelerator development in Asia were also introduced in previous papers [38–40]. As for 4GSR activity in Japan, so far, the major upgrade of SPring-8, SPring-8-II, is only a 4GSR project in Japan, which has been extensively investigated including the accelerator component R&D. SPring-8-II has been long discussed. The five-bend achromat lattice and related hardware components had been designed and developed, targeting the natural emittance of around 140 pm rad [41]. As the 3-GeV ring project started first in the country, most of efforts at SPring-8 are being focused onto the 3-GeV ring for smooth ring construction. It is expected that the SPring-8-II project will officially start soon, potentially overlapped with the 3-GeV project. For that, the lattice and related accelerator components are currently re-designed, aiming to improve the target goals. The target operational beam emittance is lower to around 80 pm rad.

HEPS is a high-performance and high-energy synchrotron radiation light source with a beam energy of 6 GeV and an ultralow emittance of better than 60 pm. HEPS mainly consists of 500 MeV linac, 454.5 m booster, storage ring, beamlines, and end-stations. In the phase I, 14
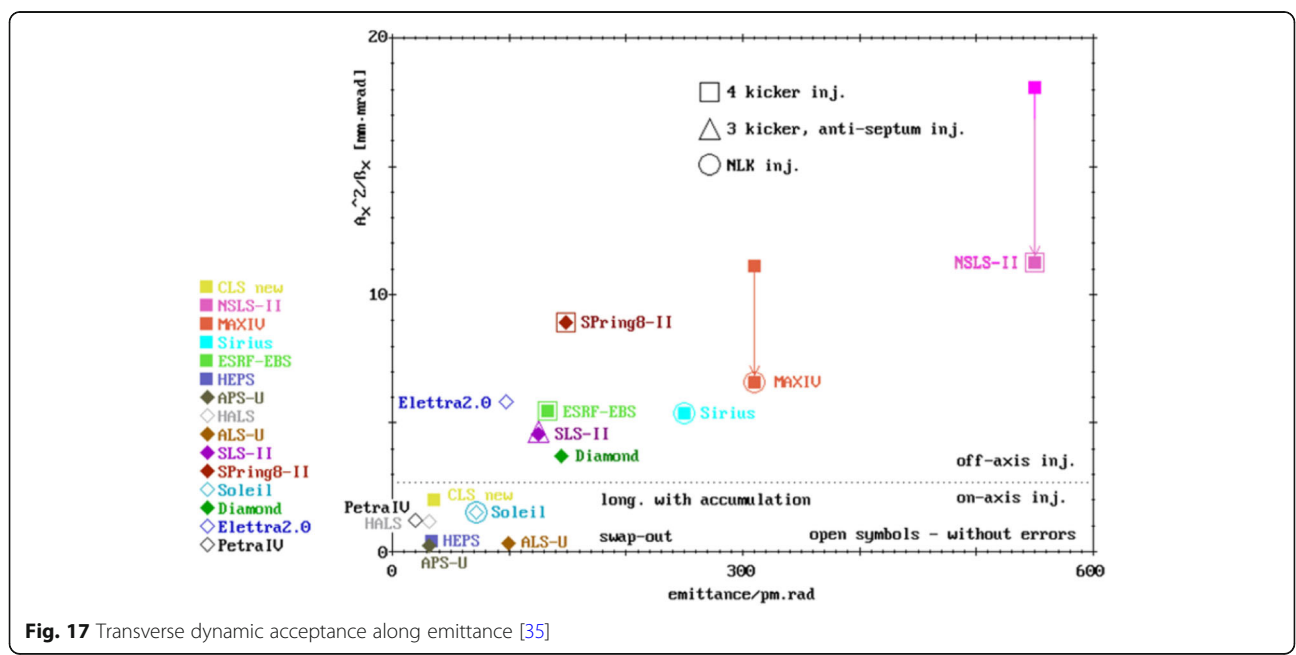

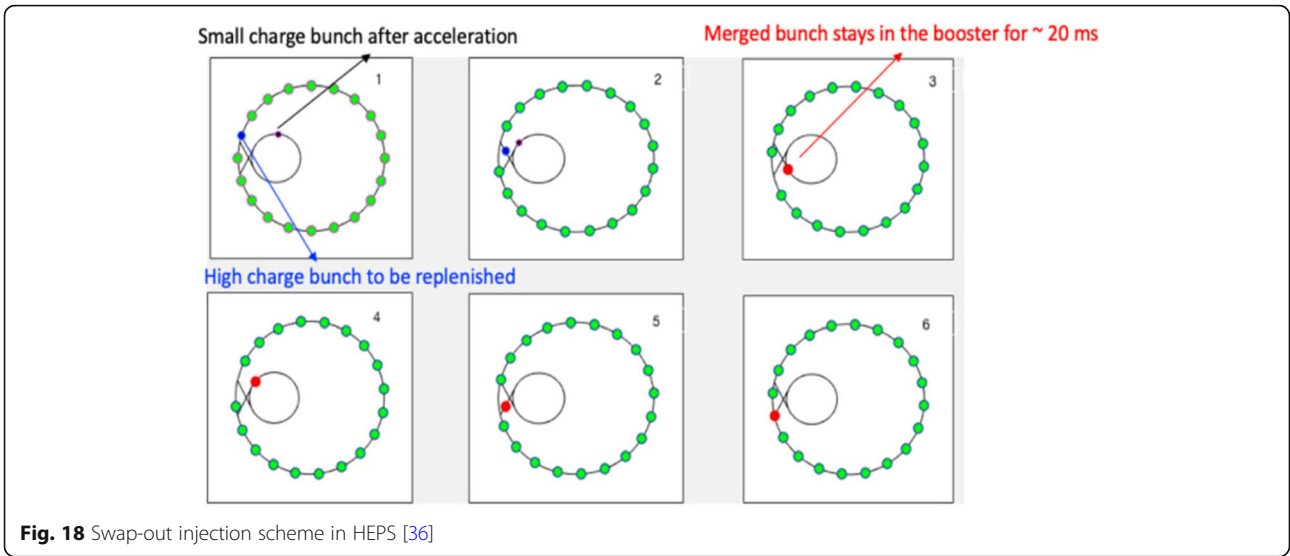**Fig. 17** Transverse dynamic acceptance along emittance [35]

Fig. 18 Swap-out injection scheme in HEPS [36]

public beamlines and corresponding experimental stations will be constructed. The storage ring of HEPS is 1360.4-m circumference, 6-GeV beam energy, and 200-mA beam current ring. The storage ring is composed of 48 modified hybrid 7 bend achromat cells. The natural emittance of HEPS is less than or equal to 60 pm. The construction of HEPS was already started and the project will be completed in 2025.

Recently Korea-4GSR [42] was officially approved and started. The CDR for Korea-4GSR had been completed and the project will be completed in 2027. The Korea-4GSR has 28 super periodic hybrid 7 bend achromat cells and the figure shows the structure and Twiss parameters of one cell of the Korea-4GSR (Fig. 21). In order to realize the worldwide competitive photon beam in 10~30 keV photon beam energy range with 800-m circumference ring, beam parameters are 4-GeV beam energy, 400-mA beam current, and 58-pm beam emittance considering well-proven technology.
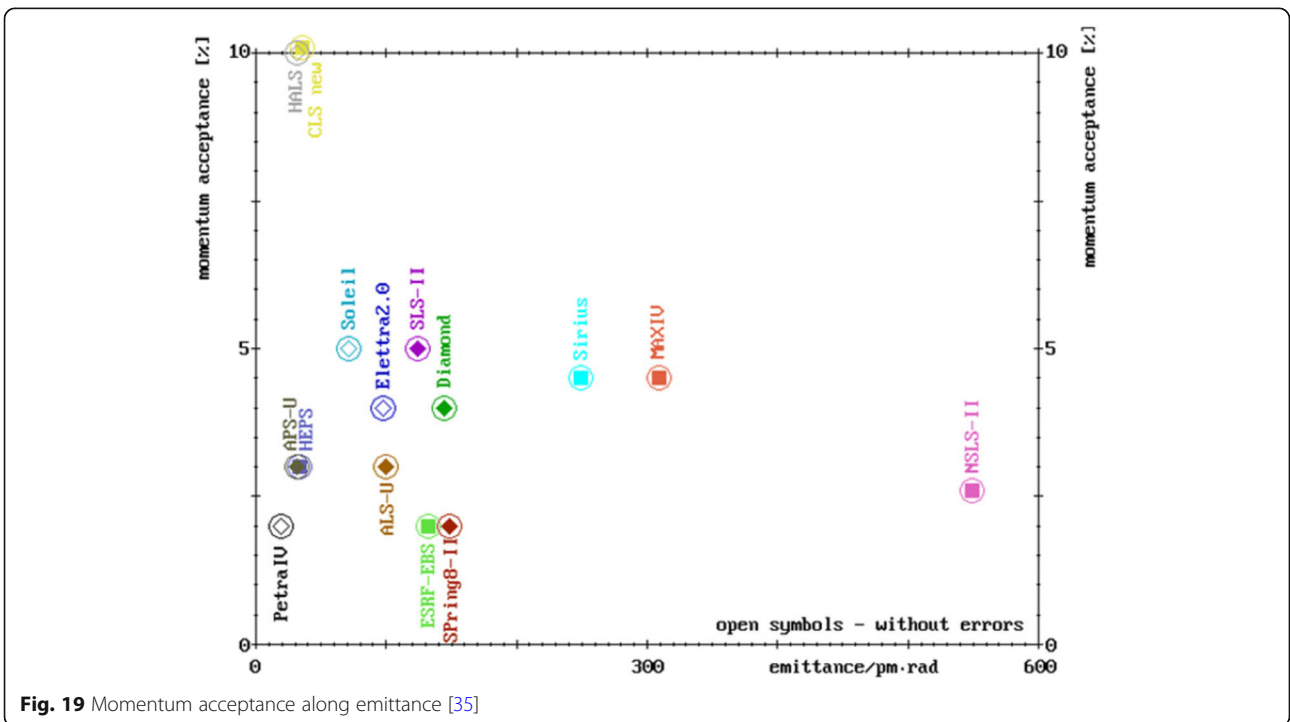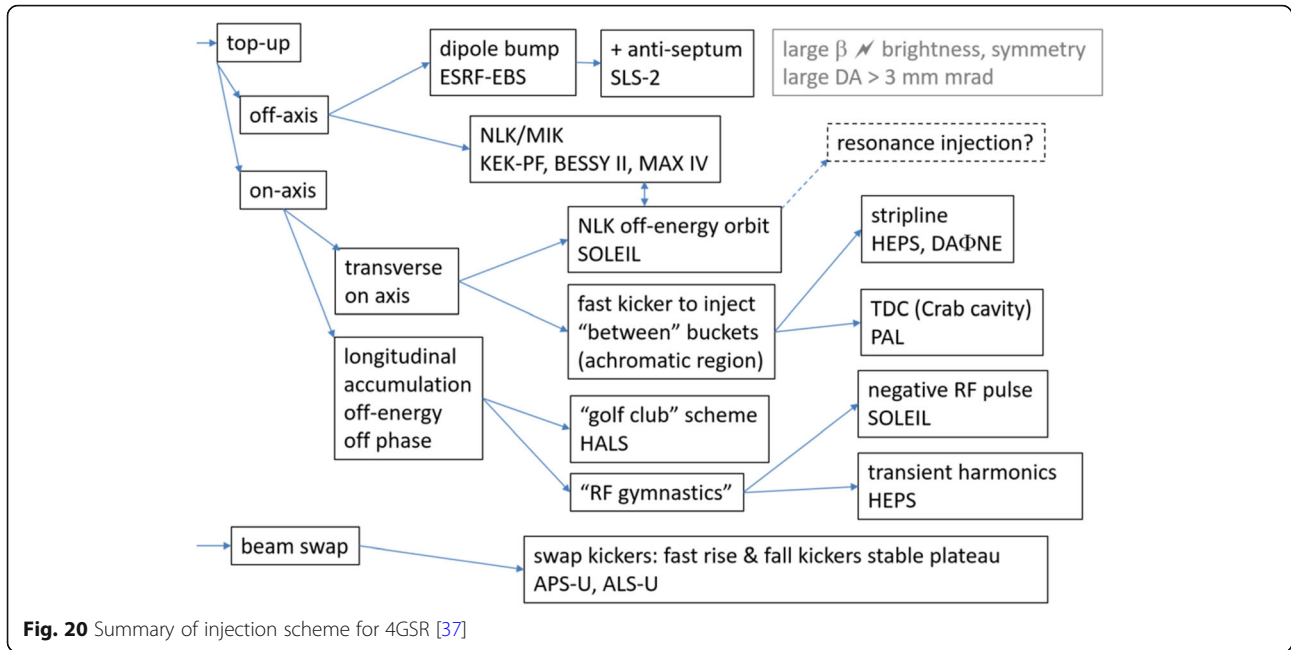

Fig. 19 Momentum acceptance along emittance [35]

Fig. 20 Summary of injection scheme for 4GSR [37]

7 Conclusion

In this paper, we survey ongoing work around the world to develop concepts and designs for fourth-generation electron storage rings. Based on the success of 3rd-generation storage ring, the 4th-generation storage ring was advent and the field is thriving. The present status of 4GSR is as follows:

– MAX-IV (Sweden) in operation (2017)

– ESRF-EBS (France) in operation (2020)
– Sirius (Brazil) in operation (2020)
– APS-U (USA) under construction and operation (2023)
– HEPS (China) under construction and operation (2025)
– ELETTRA 2.0, SLS-II, and SKIF recently funded
– PETRA-IV, ALS-U, Diamond now moved to TDR phase

Fig. 21 Lattice for Korea-4GSR [42]
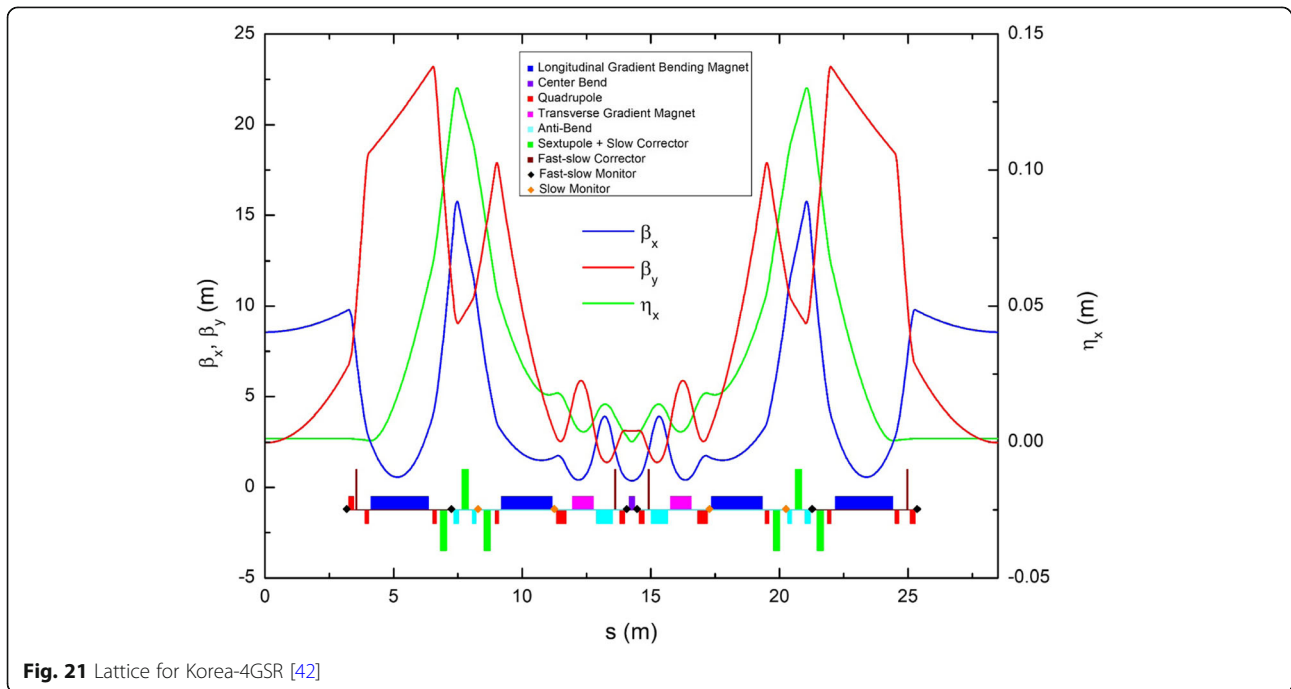
– Korea-4GSR project recently approved

Before closing this review paper, it should be mentioned that congestion of program in 2024–2025 will potentially create procurement risks to all projects [25]. Therefore, worldwide collaboration might have been needed.

Author's contributions
The author read and approved the final manuscript.

Authors' information
Seunghwan Shin is a Senior Researcher at Pohang Accelerator Laboratory and Head of the Accelerator Division in PLS-II.

Declarations

Ethics approval and consent to participate
Not applicable.

Consent for publication
Not applicable.

Competing interests
The authors declare that they have no competing interests.

References
1. SuperB workshop, https://indico.cern.ch/event/133199/contributions/125605/
2. M. Borland et al., J Synchrotron Radiat **21**, 912 (2014)
3. R. Chasman, G.K. Green, E.M. Rowe, IEEE Trans Nucl Sci **22**(3) (1975)
4. A. Jackson, Particle Accelerator. **22**, 111 (1987)
5. D. Einfeld, M. Plesko, J. Schaper, J Synchrotron Radiat **21**, 856 (2014)
6. L. Liu, N. Milas, A.H.C. Mukai, X.R. Resende, A.R.D. Rodriguet, F.H. Sa, Proc of IPAC, 1874 (2013)
7. ESRF-EBS introduction, http://indico.psi.ch/conferenceDisplay.py?confId=5589.
8. L. Emery, M. Borland, Proc of PAC, 200 (1999)
9. H.A. Padmore, ALS Light Source Note LSBL-486. September **22** (1998)
10. D.-E. Kim et al., J Korean Phys Soc **69**(6), 903 (2016)
11. EPICS, https://epics.anl.gov.
12. H. Tanaka, Proc. of the NANOBEAM2005, the 36th ICFA Advanced Beam Dynamics Workshop, Uji Campus, Kyoto University, p. 12 (2005).
13. M. Boge, et al., Proc. of PAC2005, p. 1584 (2005).
14. Francesca Curbis, et al., Proc. of FEL2014, p.549 (2014)
15. D. Einfeld and M. Plesko, Proc. of SPIE, p.201 (1993).
16. D. Einfeld and M. Plesko, Nucl. Instrum. Methods Phys. Res. A, 335, p. 402 (1993).
17. A. Wolski, Proc. of the CAS-CERN Accelerator School, CERN-2014-009, p. 245 (2014).
18. C. Steier, et al., Proc. of IPAC2014, p. 567 (2014).
19. MAX IV Detailed Design Report, https://www.maxiv.lu.se/accelerators-beamlines/accelerators/accelerator-documentation/max-iv-ddr/.
20. L. Liu, N. Milas, A. H. C. Mukai, X. R. Resende, A. R. D. Rodriguet, and F. H. Sa, Proc. of IPAC2013, p.1874 (2013)
21. ESRF-EBS: The Extremely Brilliant Source Project, http://indico.psi.ch/conferenceDisplay.py?confId=5589.
22. APS Upgrade introduction, https://www.aps.anl.gov/ APSUpgrade.
23. C. Steier et al., Proc. of IPAC 2016, p. 2956 (2016).
24. HEPS introduction, http://english.ihep.cas.cn/heps/.
25. Riccardo Bartolini, Overview of ongoing fourth-generation light source projects worldwide, https://www.maxiv.lu.se/news/7th-dlsr-2021/
26. Diamond-II introduction, https://www.diamond.ac.uk/Home/About/Vision/Diamond-II.html
27. V. Sajaev, Phys Rev AB **22**, 040102 (2019)
28. C. Herbeaux, N. Bechu, J-M. Filhol, Proc. of EPAC08, p. 3696 (2008).
29. M. Grabski, E. Al-Dmour, J Synchrotron Radiat **28**, 718 (2021)
30. R. M. Seraphim, et al., Proc. of IPAC2015, p. 2744 (2015).
31. A. Anders, et al., "Non-evaporative getter (NEG) coatings for ultrahigh vacuum in very narrow chambers", 80th IUVSTA (2016)
32. E. Belli et al., Phys Rev AB **21**, 111002 (2018)
33. Brian Norsk Jensen, MAX-IV stability task force update, Workshop on Ambient ground motion and vibration suppression for low emittance storage ring, Beijing 11 December (2017).
34. A. Xiao, M. Borland, and C. Yao, Proc. of PAC2013, p. 1076 (2013).
35. P. Kuske, *Mastering challenges of the injection into low emittance rings, ARIES-TWIIS, 3rd April* (2019)
36. G. Xu, *On-axis injection scheme for HEPS, ARIES-TWIIS, 3rd April* (2019)
37. A. Streun, *Summary present machines / beam dynamics, ARIES-TWIIS, 3rd April* (2019)
38. TAKATA, MASAKI, et al., The Next Generation 3GeV Synchrotron Radiation Facility Project in Japan. AAPPS Bull **29**, 5 (2019)
39. ZHANG YH. "Mass Measurements of Short-lived Nuclides at the Heavy-ion Storage Ring in Lanzhou." AAPPS Bull 29.5 (2019)
40. H. ZHOU, Construction of the High Intensity Heavy-ion Accelerator Facility (HIAF). AAPPS Bull **29**, 2 (2019)
41. Spring-8-II conceptual design report. http://rsc.riken.jp/eng/index.html.
42. D-E. Kim, et al., Journal of the Korean Physical Society, Vol. 78, 467 (2021).

Publisher's Note
Springer Nature remains neutral with regard to jurisdictional claims in published maps and institutional affiliations.